CHAPTER VII

STUDY OF ASSORTED INTERACTIONS OF AN IONIC LIQUID IN SIGNIFICANT SOLVENT SYSTEMS USING COMPENSATED EQUATION OF FUOSS CONDUCTANCE AND VIBRATIONAL MODE

7.1. INTRODUCTION

In recent years, ionic liquids (ILs) have attracted considerable attention owing to their potential use in a diversified range of applications. ILs are one of the most interesting and rapidly developing areas of modern physical chemistry, technologies and engineering. ILs exhibit many interesting properties, such as unique permittivity, low melting point, negligible vapour pressure, a wide liquid range, high thermal stability, high electrical conductivity and wide electrochemical window. They are used as solvents or catalysts for a variety of reactions [1, 2].

The solvation of ionic liquid in various pure non-aqueous solvents has a great demand in modern battery industry [3] and, for further more understanding, organic reaction mechanisms [4] Keeping in mind the use of ionic liquids in battery industries, here we have studied the thermodynamic and transport properties of ionic liquids in industrially important solvents. These properties provide important information about the nature and strength of intermolecular forces existing within the constituents of a solution. Fourier transform infrared (FT-IR) measurements have also been done as it is one of the most convenient methods to investigate the molecular interactions in electrolytic solutions.

There are several imidazolium-, pyridinium-, ammonium- and phosphonium-based cation ionic liquids commercially available. Compared with other ILs, the phosphonium-based ILs are less toxic, thermally more stable and readily available in bulk quantities and less expensive [5]. Phosphonium ILs have several advantages over other types of ILs, including, in specific cases and applications, higher thermal stability, lower

Published in *Ionics*, 2014, 20, 1001-1009

viscosity and higher stability in strongly basic or strongly reducing conditions. Phosphonium-based ILs is now appearing in applications as phase transfer catalysts [6], organic synthesis and electrochemical media.

The non-aqueous system has been of immense importance [7] to the technologist and theoretician as many chemical processes occur in these systems to examine the nature and magnitude of ion-ion and ion-solvent interactions. Conductance study is a very important tool in obtaining the information regarding the solvation and association behaviour of ions in solution. FT-IR spectroscopy has also been one of the most convenient methods for investigating the ion–solvent interactions in electrolytic solutions [8, 9, 10].

In this work, an attempt has been made to explore the electrolytic properties of [Bu_4PMS] (solid phase) in selected industrially important solvents. Here, we have investigated the conductance behaviour of [Bu_4PMS] in dimethyl sulphoxide (DMSO), N, N-dimethyl acetamide (DMA) and N, N-dimethyl formamide (DMF) at 298.15 K. These solvents used in the study are industrially very important. FT-IR spectroscopy of the salt in these solvents gives the information about the molecular interaction occurring in these systems.

7.2. EXPERIMENTS

7.2.1. *Source and purity of samples*

Ionic liquid tetrabutylphosphonium methanesulfonate [Bu_4PMS] of puriss grade was procured from Aldrich, Germany and was used as purchased. The mass fraction purity of [Bu_4PMS] was ≥ 0.98.

All the solvents (DMSO, DMA and DMF) of spectroscopic grade were procured from Merck, India. These were further purified by standard methods [11]. The values of their mass fraction purities of the solvents were ≥ 0.99. See Table 1.

7.2.2. *Apparatus and Procedure*

A stock solution of the electrolyte was prepared by mass (weighted with Mettler Toledo AG-285 with uncertainty ± 0.0003 g), and the working solutions were obtained by mass dilution at 298.15 K. Uncertainty of molarity of different salt solutions is evaluated to be ±0.0001 mol·dm^{-3}. A vibrating U-tube digital density meter (DMA 4500M, Anton Paar) with an accuracy of ±0.00005 g cm^{-3} was used to measure the densities of the solutions (ρ) after being calibrated by triply distilled water and passing dry air. The temperature was fixed within ±0.01 K.

The viscosity was also measured with the help Brookfield DV-III Ultra Programmable Rheometer with spindle size 42 fitted to a Brookfield Digital Bath TC-500.

The conductance measurements were carried out in a Systronic-308 conductivity meter (accuracy ±0.01) using a dip-type immersion conductivity cell, CD-10, having a cell constant of approximately 0.1 ±0.001 cm^{-1}. Measurement was made in a water bath maintained within T = 298.15 ± 0.01 K, and the cell was calibrated by the method proposed by Lind et al [12]. The conductance data were reported at a frequency of 1 kHz.

Infrared spectra were recorded on an 8300 FT-IR spectrometer (Shimadzu, Japan). The details of the instrument have already been previously described [10].

7.3. RESULTS AND DISCUSSION

7.3.1. *Electrical Conductance*

7.3.1.1. *Ion-pair formation:*

The physical properties of the pure solvent at 298.15 K are reported in Table 2. The molar conductance (Λ) has been obtained from the specific conductance (κ) value using the following equation [13]

$$\Lambda = (1000\,\kappa)/c \qquad (1)$$

where c is the molar concentration and κ is the measured specific conductance of the studied solution. The experimental values of molar conductances (Λ) of ionic liquid [Bu_4PMS] measured at the corresponding molar concentrations (c) in different studied

solvents are plotted in Figure 1. Linear conductance curves (Λ versus $\sqrt{c}$) were obtained (Figure 1) for the electrolyte in dimethylsulfoxide, dimethylacetamide and dimethylformamide, and extrapolation of $\sqrt{c} = 0$ evaluated the starting limiting molar conductance for the electrolytes. The conductance results for ion-pair formation have been analysed using the Fuoss conductance equation [14,15]. Thus, with a given set of conductivity values $(c_j, \Lambda_j, j=1,...n)$ three adjustable parameters, *i.e.* Λ_o, K_A and R have been derived from the Fuoss equation. Here, Λ_o is the limiting molar conductance, K_A is the observed association constant and R is the association distance, i.e. the maximum centre-to-centre distance between the ions in the solvent-separated ion-pairs. There is no precise method [16] for determining the R value, but in order to treat the data in our system, R value is assumed to be $R = a + d$, where $a = (r_+ + r_-)$ is the sum of the crystallographic radii of the ions and d is the average distance corresponding to the side of a cell occupied by a solvent molecule. The distance, d, is given by [17]

$$d\,(\text{Å}) = 1.183\,(M/\rho)^{1/3} \tag{2}$$

where M is the molar mass and ρ is the density of the solvent.

Thus, the Fuoss conductance equation may be represented as follows:

$$\Lambda = P\Lambda_o[(1+R_X)+E_L] \tag{3}$$

$$P = 1-\alpha(1-\gamma) \tag{4}$$

$$\gamma = 1-K_A c\gamma^2 f^2 \tag{5}$$

$$-\ln f = \beta\kappa/2(1+\kappa R) \tag{6}$$

$$\beta = e^2/(\varepsilon k_B T) \tag{7}$$

$$K_A = K_R/(1-\alpha) = K_R/(1+K_S) \tag{8}$$

where R_X is the relaxation field effect, E_L is the electrophoretic counter current, κ is the radius of the ion atmosphere, ε is the dielectric constant of the solvents, e is the electron charge, c is the molarity of the solution, k_B is the Boltzmann constant, K_A is the overall paring constant, K_S is the association constant of the contact pairs, K_R is the association constant of the solvent-separated pairs, γ is the fraction of solute present as unpaired ion, α is the fraction of contact pairs, f is the activity coefficient, T is the absolute temperature and β is twice the Bjerrum distance.

The computations were performed using the program suggested by Fuoss. The initial Λ_o values for the iteration procedure are obtained from Shedlovsky's extrapolation of the data [18]. Input for the program is the no. of data, n, followed by ε, η (viscosity of the solvent), initial Λ_0 value, T, ρ (density of the solvent), mole fraction of the first component, molar masses, M_1 and M_2 along with c_j, Λ_j values where $j = 1, 2.....n$ and an instruction to cover preselected range of R values.

In Practice, calculations are performed by finding the values of Λ_0 and α which minimize the standard deviation, δ:

$$\delta^2 = \sum[\Lambda_j(cal) - \Lambda_j(obs)]^2 / (n-m) \qquad (9)$$

where n is the number of experimental points and m is the number of fitting parameters. The conductance data have been explained and discussed by fixing the distance of closest approach R with two parameter fit (m = 2). For a sequence of R values and then plotting δ against R, the best-fit R corresponds to the minimum of the δ-R versus R curve. Thus, an approximated sum is made over a fairly wide range of R values using 0.1 increment to locate the minimum, but no significant minima is found in the δ-R curves; thus, R values are assumed to be $R = a + d$, with terms having usual significance. Finally, the corresponding Λ_0 and K_A values are obtained which are reported in Table 3 along with R and δ for all the solutions.

A perusal of Table 3 shows that the limiting molar conductance (Λ_0) of [Bu_4PMS] is highest in the case of DMF and lowest in the case of DMSO among the studied solvents. The trend of the Λ_0 of the electrolytes in three different solvents is as follows:

DMF > DMA > DMSO.

Table 3 also implies that the association constant (K_A) of the [Bu_4PMS] is greater in DMSO than in DMA than in DMF. Hence, there is greater ion-solvent interaction in DMSO than in DMA than in DMF, leading to a lower conductance of [Bu_4PMS] in the former than the latter two. This shows that [Bu_4PMS] is solvated more by DMSO, which has the highest viscosity value among the studied solvents. The highest ion-solvent interaction leading to very high ion-solvation is seen in case of DMSO which is evident

from the K_A values given in Table 3. The weakest ion-solvation is seen in the case of DMF. The trend in Λ_o and ion-association can also be discussed through another characteristic function called the Walden product ($\Lambda_o\eta$, the limiting molar conduactance-solvent viscosity product) is a constant under normal condition; given in Table 3. Table 3 shows that the decreasing trend of Walden's function is mainly in agreement with the concomitant decrease of solvent viscosity and increase of limiting molar conductance for the electrolyte (IL) in the solvents. This is also justified as the Walden product of an ion or solute which is inversely proportional to the effective solvated radius (r_{eff}) of the ion or solute in a particular solvent/solvent mixture [19] :

$$\Lambda_0\eta = \frac{1}{6\Pi r_{eff} T} \tag{10}$$

This points out to the fact that the electrostatic ion-solvent interaction or ion-association is strong in these cases. The variation of the Walden product reflects the change of solvation [20] though the variation of the Walden product with solvent composition is difficult to interpret quantitatively, but its variation with solvent composition can still be explained by

1. *Preference to solvation of IL for solvent molecules*: Taking into consideration of the conductance and association constant value of ionic liquid in different solvents, we can say that the IL mostly prefers the dimethylsulfoxide among the other studied solvents, and the order of preference by the IL in the solvents is as follows:

   dimethyl sulfoxide > N,N-dimethyl acetamide
   > N,N-dimethyl formamide.

2. *Considering the structural aspect of the solvents*: Polar aprotic solvents (e.g. DMF, DMA, DMSO) dissolve ionic compounds and solvate cations very well. They do not solvate anions to any appreciable extent because they cannot form H-bonds and having positive centres are well shielded from any interaction with anions. When the ionic liquid [Bu_4PMS] is dissolved in the abovementioned polar aprotic solvents, the following interaction may be observed:

(a) In the case of solvent DMF, the only interaction present is the between negatively charged oxygen atom of DMF and positively charged P atom of $[Bu_4P]^+$, as shown in (I).

(b) The same type of interaction is present in the case of solvent DMA (II); here, the interaction is more intense due to the presence of methyl ($-CH_3$) group which pushes electrons towards oxygen, making it more negative for stronger interaction.

(c) In the case of DMSO as solvent, two types of interaction shown in (III) are possible: (i) between the negatively charged oxygen atom of DMSO and positively charged P atom of $[Bu_4P]^+$, and (ii) between positively charged S atom of DMSO and negatively charged S atom of [MS]. The interaction (ii) is only possible because the S atom is larger than the N atom and is less shielded by two methyl groups compared to N atom in the case of DMF and DMA. For these reason, there is more conductance of $[Bu_4PMS]$ in DMF than DMA and DMSO. Hence, lower the conductance, the greater is the interaction/association, which is in the following order: DMSO > DMA > DMF

The schematic representation of ion-solvent interaction for the particular ion in the studied solvent is depicted in **Scheme 1.**

The starting point for most evaluations of ionic conductance is Stokes' law which states that the limiting Walden product ($\lambda_0^{\pm}\eta_0$; product of the limiting ionic conductance and solvent viscosity) for any singly charged spherical ion is a function of the ionic radius only, and thus, under normal conditions is a constant. The values of the ionic conductances $\lambda_o^{\pm}$ (for the Bu_4P^+ cation and MS^- anion) in different solvents DMSO, DMA and DMF, were calculated using tetrabutylammonium tetraphenylborate (Bu_4NBPh_4) as a 'reference electrolyte' following the scheme as suggested by B. Das et al. [20].

The ionic limiting molar conductances $\lambda_o^{\pm}$ for $[Bu_4PMS]$ in all the solvents have been calculated by interpolation of conductance data from the literature [21] using cubic spline fitting. Table 4 shows that the greater share of the conductance values comes

from the anion MS^- than the cation $[Bu_4P]^+$. The $\lambda_o^{\pm}$ values were in turn utilised for the calculation of Stokes' radii (r_s) according to the classical expression [22]:

$$r_S = \frac{F^2}{6\pi N_A \lambda_o^{\pm} r_c} \tag{11}$$

Ionic Walden's function $\lambda_o^{\pm}\eta$, Stokes' radii r_s, and crystallographic radii r_c are presented in Table 4. The trends in Walden products $\Lambda_o\eta$ and ionic Walden products $\lambda_o^{\pm}\eta_o$ for the electrolytes in the solvents DMSO, DMA and DMF are depicted in Tables 3 and 4, respectively. They indicate that both the ionic Walden products $\lambda_o^{\pm}\eta$ and Walden products $\Lambda_o\eta$ for the electrolyte are greater in the case of DMSO than in DMA and DMF. For the Bu_4P^+ and MS^- ions, the Stokes' radii r_s are either lower or comparable to their crystallographic radii r_c; this suggests that the ion is comparatively less solvated than alkali metal ions due to its intrinsic low surface charge density. The distance parameter R, shown in Table 3, is the least distance that two free ions can approach together before they merge into an ion pair.

The nature of the curve for the Gibbs energy changes for ion-pair formation, ΔG^o, clearly predicts the tendency for ion-pair formation. The Gibbs energy change ΔG^o is calculated by the following relationship [23] and is given in Table 3:

$$\Delta G^o = - RT \ln K_A \tag{12}$$

The negative values of ΔG^o can be explained by considering the participation of specific interaction in the ion association process. It is observed from the Table 3 that the values of the Gibbs free energy are all negative, all over the solutions and the negativity increases from dimethylformamide to dimethylsulfoxide. The increasing negativity in the value of ΔG^o of $[Bu_4PMS]$ leads to the increase in the ion-solvent interaction. This result indicates the extent of solvation enhanced by the following order:

DMSO > DMA > DMF

This is an excellent agreement with the observation obtained from conductance values discussed earlier in this paper.

The diffusion coefficient (D) is obtained using the Stokes-Einstein relation:

$$D=\frac{kT}{6\pi\eta r_s} \tag{13}$$

where k is the Boltzmann's constant, T is the temperature, η is the solvent viscosity and r_s is the Stoke's radii.

The ionic mobility was obtained using the following equation:

$$i=\frac{z^{+}F}{RT}D \tag{14}$$

where $z_{\pm}$, F, R, T and D is the ionic charge, Faraday constant, universal gas constant, temperature, and diffusion coefficient, respectively. Table 5 shows that the diffusion coefficient of MS^- is more than Bu_4P^+ in all the solvents which indicates that MS^- ion diffuses more in the solvents. The diffusion coefficient decrease from DMF to DMSO as indicated in Table 5 for both $[Bu_4P]^+$ and MS^- ions showing greater diffusion of the ions in DMF. At the same time, the ionic mobility values given in Table 5 also shows that the mobility of MS^- is higher than that of $[Bu_4P]^+$ in all the investigated solvents because of its smaller size than that of cation. Hence, the greater share of the conductance comes form the anions than the cation.

7.3.1.2. *FT-IR Spectroscopic Study*

With the help of FT-IR spectroscopy, the molecular interaction existing between the solute and the solvent can be studied. The concentration of the studied solutions used in the IR study is 0.05 M, the IR spectra of the pure solvents were studied.

The stretching frequencies of the characteristic groups are given in Table 6 and Figures 2, 3, and 4. In the case of DMF, a sharp peak is obtained at 1,674.6 cm^{-1} which is attributed to the C=O stretching vibration range (1,630-1,690 cm^{-1}). The peak shifts to 1,700.2cm^{-1} due to the interaction of $[Bu_4P]^+$ /MS^- ion with the C=O dipole showing ion-dipole interaction which is formed due to the disruption of H-bonding interaction in DMF molecules [24].

The IR spectra of DMA shows a sharp peak at 1,748.4 cm^{-1} for C=O stretching vibration range (1,680-1,750 cm^{-1}). When the IR spectra of $[Bu_4PMS]$+DMA solution was taken,

the peak shifted to 1,783.2 cm^{-1} leading to ion-dipole interaction between $[Bu_4P]^+$ /MS^- and C=O dipole.

The greatest interaction is seen between [Bu_4PMS] and DMSO as evidenced from the values of the K_A obtained from the conductivity studies. In the case of DMSO, a peak is obtained at 1,026.0 cm^{-1} since S=O stretching vibration (range 1,030-1,060 cm^{-1}) shifts to 1,077.4 cm^{-1} by the addition of [Bu_4PMS] to DMSO leading to the disruption of weak H-bonding interaction between the two DMSO molecules [25] and formation of ion-dipole interaction between $[Bu_4P]^+$ /MS^- and S=O dipole.

Table 6 shows that the Δν values increases from N,N-dimethyl formamide to dimethylsulfoxide, i.e. the shift in stretching frequency increases from N,N-dimethyl formamide to dimethylsulfoxide. The order of Δν obtained from the FTIR spectra is

DMF< DMA < DMSO

The greater the value of Δν, there is attraction between the electrolyte (IL) and solvent molecules. Therefore, with the increase in the value of Δν, the distance between the electrolyte and the solvent molecules decreases. Thus, the ion-solvent interaction increases with the increase in Δν values from N,N-dimethyl formamide to dimethylsulfoxide. Thus, DMSO stabilises the electrolytes (ion-solvent interaction) to a greater extent than dimethylacetamide, which in turn stabilises the same greater than dimethylformamide. Therefore, the obtained result is in line with the conductivity study which was discussed earlier.

A schematic representation of the interaction occurring in pure solvent and [Bu_4PMS] + Solvent together with the trend in the ion solvation in the studied solvents has been shown in **Scheme 2.**

7.4. CONCLUSIONS

The present work reveals an extensive study on the ion solvation behavior of the tetrabutylphosphonium methanesulfonate [Bu_4PMS] in DMSO, DMA and DMF through the conductometric and FTIR measurements. From the study, it becomes clear that the salt is more associated with DMSO than the other solvents. It can also be seen that in the

conductometric studies in DMSO, DMA and DMF, the electrolyte remains as ion pairs. The ionic conductivity values suggest the fact that the anions (MS^-) conduct more than the cation $[Bu_4P]^+$. The diffusion coefficient and ionic mobility also show that in studied ionic liquid, the anions diffuses more due to high ionic mobility compared to the cation because the size of the anion is smaller than that of the cation. In all the solvents, the electrolyte forms ion-dipole interactions as evidenced from the FT- IR studies.

Published in *Ionics,* 2014, 20, 1001-1009

REFERENCES

[1]. T. Welton, *Chem. Rev.* 99 (**1999**) 2071.

[2]. J.S. Wilkes, *J. Mol. Catal A .Chem.* 214 (**2004**) 11-17.

[3]. D. Aurbach, *Non-aqueous Electrochemistry*, Marcel Dekker, Inc: New York, (**1999**).

[4]. J.A. Krom, J.T. Petty, A. Streitwieser, *J. Am. Chem. Soc.* 115 (**1993**) 8024.

[5]. F. Atefi, M.T. Garcia, R.D. Singer, P.J. Scammells, *Green. Chem.* 11(**2009**) 1595.

[6]. T. Ramnial, D.D. Ino, J.AC. Clyburne, *Chem. Commun.* (**2005**) 325.

[7]. O. Popvych, R.P.T. Tomkins, *Nonaqueous Solution Chemistry*, Chapter 4. Wiley-Interscience: New York (**1981**).

[8]. R.R. Dogonadze, E. Kalman, A. A. Kornyshev, J. Ulstrup, *The Chemical Physics of Solvation, Part B, Spectroscopy Solvation*: Elsevier Amsterdam (**1986**).

[9]. A. Sinha, G. Ghosh, M.N. Roy, *J. Phys. Chem. Liqs.* 48 (**2010**) 62-78.

[10]. A. Sinha, A. Bhattacharjee, M.N. Roy, *J. Disp. Sc. Techn.* 30 (**2009**) 1003.

[11]. D.D. Perrin, W.L.F. Armarego, *Purification of Laboratory Chemicals*, third ed. pp. 299. Pergamon Press: Oxford (**1988**).

[12]. J.E. Jr. Lind, J.J. Zwolenik, R.M. Fuoss, *J. Am. Chem. Soc.* 81(**1959**) 1557.

[13]. F.I. El-Dossoki, *J. Mol. Liq.* 151(**2010**) 1.

[14]. R.M. Fuoss, *Proc. Natl. Acad. Sci. U.S.A.* 75(**2010**) 16.

[15]. R.M. Fuoss, *J. Phys. Chem.* 82 (**1978**) 2427.

[16]. B. Per, *Acta. Chem. Scand. A.* 31(**1977**) 869.

[17]. R.M. Fuoss, F. Accascina, Electrolytic Conductance, Interscience: New York (**1959**).

[18]. D.S. Gill, M.S. Chauhan, *Z. Phys. Chem. NF.* 140 (**1984**) 139.

[19]. J. Bhat. Ishwara, P. Bindu, *J. Ind. Chem. Soc.* 72 (**1995**) 783.

[20]. J.M. Chakraborty, B. Das, *Z. Phys. Chem.* 218 (**2004**) 219.

[21]. R.M. Fuoss, E. Hirsch, *J. Am. Chem. Soc.* 82(**1960**) 1013.

[22]. R.A. Robinson, R.H. Stokes, *Electrolyte Solutions*, Chapter 6, pp. 130. Butterworth: London (**1959**).

[23]. R.M. Fuoss, C.A. Kraus, *J. Am. Chem. Soc.* 55 (**1933**) 2387.

[24]. C. Desfrancois, V. Periquet, S. Carles, J.P. Schermann, L. Adamowicz, *j. Chem. Phys.* 239 (**1998**) 475.

[25]. O. Shun-Li, W. Nan-Nan, L. Jing-Yao, S. Cheng-Lin, L. Zuo-Wei, G. Shu-Qin, *Chin. Phys. B.* 19 (**2010**) 123101.

[26]. T.M. Aminabhavi, B. Gopalakrishna, *J. Chem. Eng. Data.* 40(4) (**1995**)856. .

[27]. A.K, Covington, T. Dickinson, Physical chemistry of organic solvent systems, Plenum: New York (**1973**).

[28]. P.R. Philip, C. Jolicoeur, *J. Phys. Chem.* 77(**1973**) 3071.

[29]. S.S. Smith, E.D. Steinle, M.E. Meyerhoff, D.C. Dawson, *J Gen Physiol.* 114 (**1999**) 799.

TABLES

Table 1. Sample description

Chemical name	Source	Initial mass fraction purity	Purification method	Final mass fraction purity
[Bu_4PMS]	Sigma-Aldrich, Germany	0.98	Used as procured	0.98
DMSO	Merck, India	0.98	Purified by standard methods [11]	0.99
DMA	Merck, India	0.98	Purified by standard methods [11]	0.99
DMF	Merck, India	0.98	Purified by standard methods [11]	0.99

Table 2. Values of Density (ρ), Viscosity (η) and Dielectric constant (ε_r) of pure solvents at T = 298.15 K

Solvents	$\rho^a \times 10^{-3}$(kg m^{-3})		η^b(mPa s)		ε_r
	Expt	Lit	Expt	Lit	
DMSO	1.09602	1.09600 [26]	1.95	1.948 [26]	46.70 [27]
DMA	0.93680	0.93660 [26]	0.92	0.920 [26]	37.78 [27]
DMF	0.94450	0.94450 [26]	0.79	0.796 [26]	36.71[27]

For T, uncertainity in the temperature values: ± 0.01 K
[a] uncertainity in density values is ± 0.00005 g cm^{-3}.
[b] uncertainity in viscosity values is ± 0.03 mPa s.

Table 3. Limiting molar conductivity (Λ_0), the association constant (K_A), the distance of closest approach of ions (R), standard deviations δ of experimental Λ from equation 1, Walden product ($\Lambda_0\eta$) and Gibb's energy change (ΔG^o) of [Bu_4PMS] in studied solvent systems at T = 298.15 K

Solvents	$\Lambda_o \times 10^4$ (S m^2 mol^{-1})	K_A (dm^3 mol^{-1})	R (Å)	δ	$\Lambda_o\eta \times 10^4$ (S m^2 mol^{-1} mPa s)	Log(K_A)	ΔG^0 (kJ mol^{-1})
DMSO	33.97	29.89	12.66	0.13	66.11	5.48	-3.12
DMA	51.31	17.36	13.11	0.12	47.36	5.24	-2.99
DMF	57.07	12.68	12.79	0.17	45.31	5.10	-2.91

Published in *Ionics*, 2014, 20, 1001-1009

Table 4. Limiting ionic conductance ($\lambda_o^{\pm}$), ionic Walden product ($\lambda_o^{\pm}\eta$), Stokes' radii (r_S) and crystallographic radii (r_C) of [Bu_4PMS] in studied at T = 298.15 K

Solvents	Ion	$\lambda_o^{\pm}$ (S m² mol⁻¹)	$\lambda_o^{\pm}\eta$ (S m² mol⁻¹ mPa s)	r_S (Å)	[a]r_C (Å)
DMSO	Bu_4P^+	13.26	25.80	3.18	4.42
	MS^-	20.71	40.30	2.03	2.83
DMA	Bu_4P^+	20.03	18.49	4.43	4.42
	MS^-	31.28	28.87	2.84	2.83
DMF	Bu_4P^+	22.28	17.69	4.63	4.42
	MS^-	34.79	27.63	2.97	2.83

[a] Crystallographic radii for cation from [28] and for anion calculated and judged from Ref. [29], respectively

Table 5. Diffusion Coefficient (D) and ionic mobility (i) of $[Bu_4P]^+$ and MS^- in studied solvents at 298.15 K

Solvents	$D \cdot 10^{10}$/(m² s⁻¹)		$i \cdot 10^8$/(m² s⁻¹ volt⁻¹)	
	Bu_4P^+	MS^-	Bu_4P^+	MS^-
DMSO	3.53	5.52	1.38	2.15
DMA	5.34	8.33	2.08	3.24
DMF	5.94	9.27	2.31	3.61

Table 6. Stretching frequencies of the functional groups present in the pure solvent and change of frequency after addition of IL, [Bu_4PMS] in the solvents.

Solvents	Stretching frequencies				
	Functional Group	Range (ν cm⁻¹)	Pure Solvent (ν_o cm⁻¹)	[Bu_4PMS]+Solvent (ν_s cm⁻¹)	$\Delta\nu$ (cm⁻¹)
DMF	(aldehydic) C=O	1630-1690	1674.6	1700.2	25.6
DMA	(carbonyl) C=O	1680-1750	1748.4	1783.2	34.8
DMSO	S=O	1030-1060	1026.0	1077.4	51.4

FIGURES

Figure 1. Plot of molar conductance (Λ) and the square root of molar concentration ($\sqrt{c}$) of [Bu_4PMS] in DMSO (*black diamond*), DMA (*black traingle*), and DMF (*black circle*), respectively, at T = 298.15 K

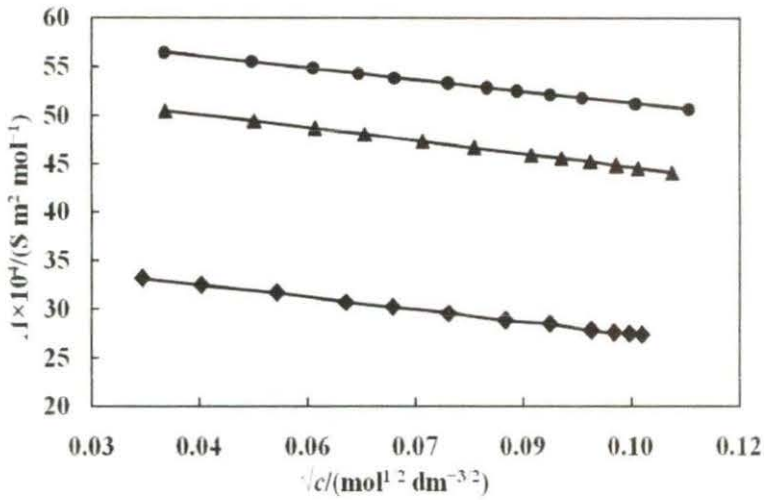

Figure 2. Stretching frequency of C-O in DMF (*black solid line*) and [Bu_4PMS] + DMF (*red solid line*).

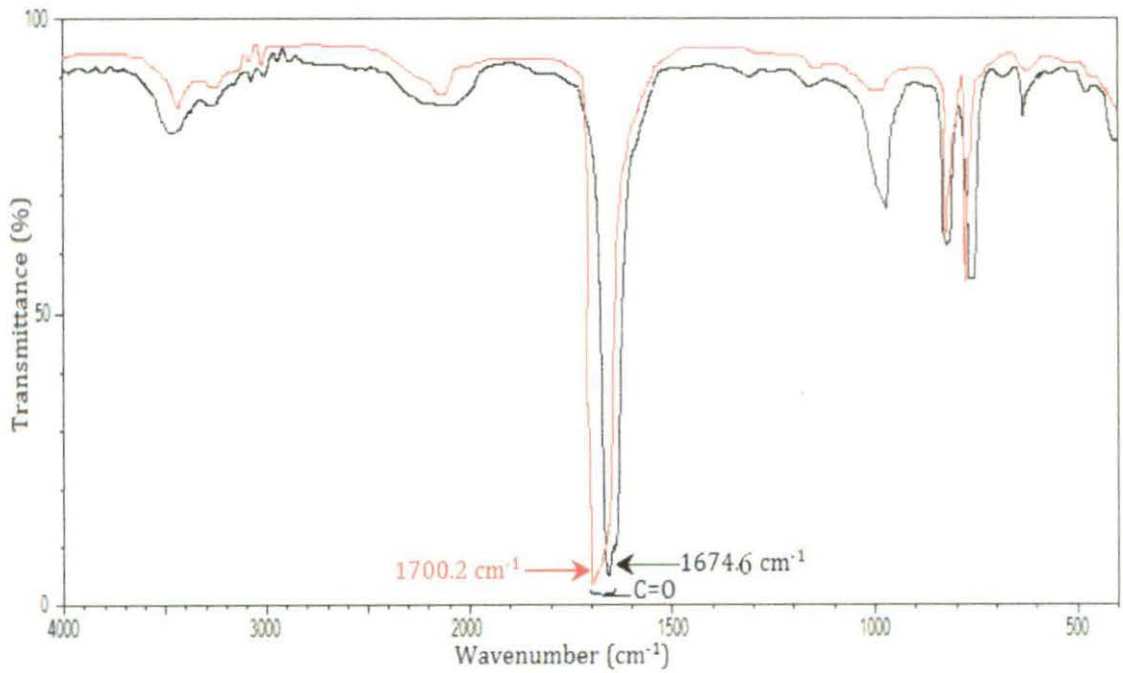

Figure 3. Stretching frequency of C-O in DMA (*black solid line*) and [Bu_4PMS] + DMA (*red solid line*).

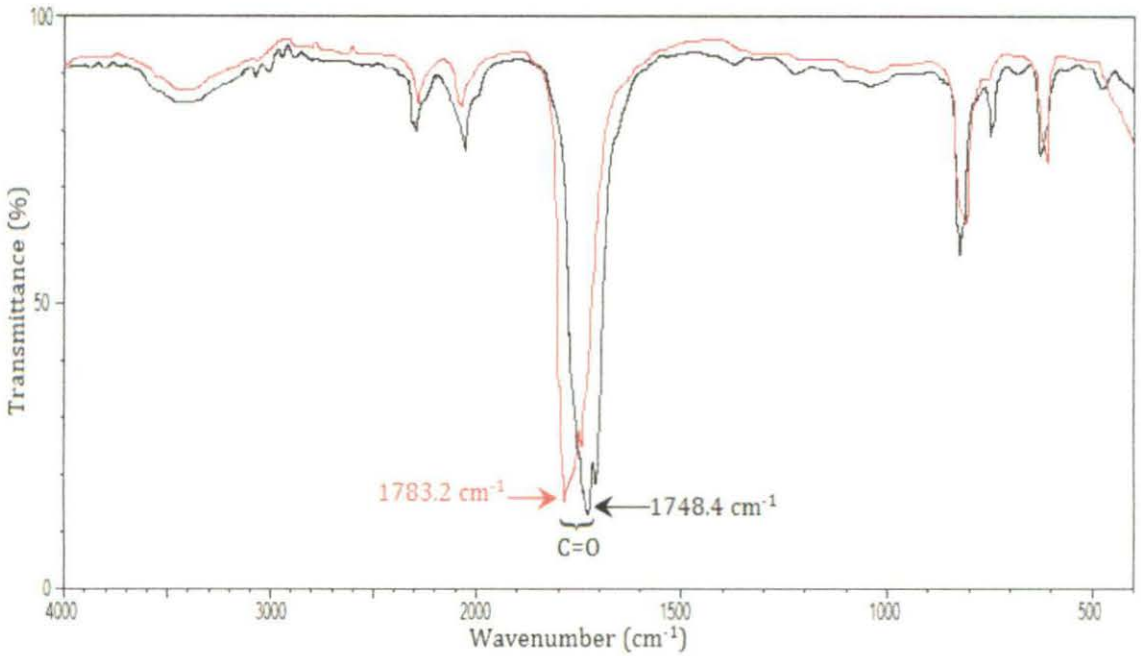

Figure 4. Stretching frequency of S=O in DMSO (*black solid line*) and [Bu_4PMS] + DMSO (*red solid line*).

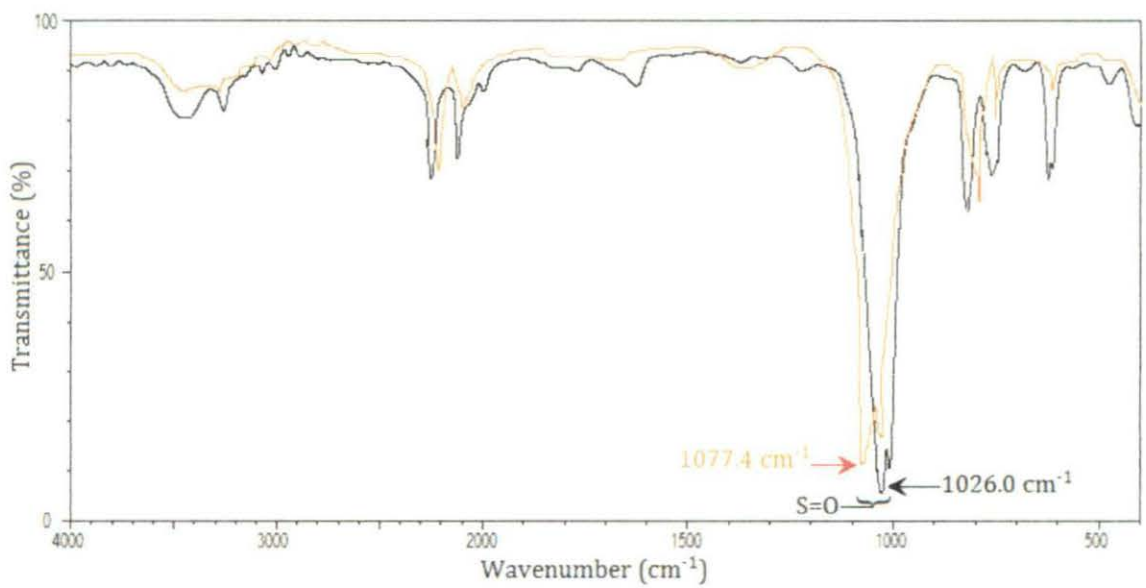

SCHEMES

Scheme 1. The schematic representation of ion solvation for the particular ion in the studied solutions {[Bu_4PMS] +solvents}

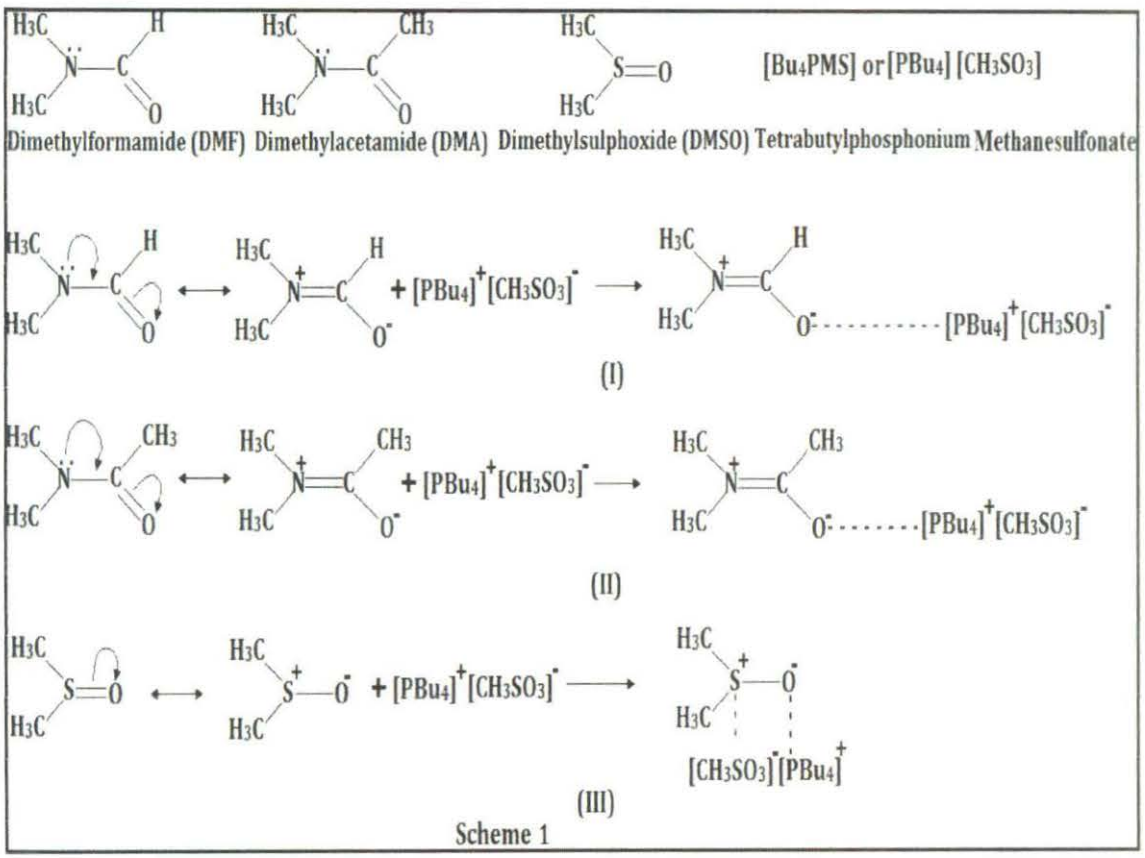

Scheme 1

Scheme 2. Schematic representation of the interaction occurring in pure solvent and {[Bu_4PMS] +solvents} together with the trend in the ion solvation in the studied solvent which is as follows: DMF <DMA < DMSO